CONSTRUCTION OF SHIFT-ORTHOGONAL WAVELETS USING SPLINES

Michael Unser, Philippe Thévenaz, and Akram Aldroubi

Biomedical Engineering and Instrumentation Program, Bldg. 13, Room 3N17,
National Center for Research Resources, National Institutes of Health,
Bethesda, Maryland 20892-5766, USA.

ABSTRACT

We present examples of a new type of wavelet basis functions that are orthogonal across shifts, but not across scales. The analysis functions are low order splines (piecewise constant or linear) while the synthesis functions are polynomial splines of higher degree n_2. The approximation power of these representations is essentially as good as that of the corresponding Battle-Lemarié orthogonal wavelet transform, with the difference that the present wavelet synthesis filters have a much faster decay. This last property, together with the fact that these transformations are almost orthogonal, may be useful for image coding and data compression.

Keywords: splines, wavelet basis, biorthogonal wavelets, perfect reconstruction filterbanks, approximation properties, image coding.

1. INTRODUCTION

So far, researchers in wavelet theory have identified and characterized three primary types of multiresolution bases of L_2 (the space of square integrable functions) [8, 9, 11, 22]. The first and earlier type are the orthogonal wavelet bases (e.g., Daubechies, and Battle-Lemarié wavelets) [7, 11]. The second closely related family are the semi-orthogonal wavelets which span the same multiresolution subspaces as before, but are not necessarily orthogonal with respect to shifts [4, 19]. The versatility of semi-orthogonal wavelet basis allows one to introduce many interesting properties [4, 19], and almost any desirable shape [1], while retaining the orthogonality property across scales that is inherent to Mallat's construction. A noteworthy example in this category are the B-spline wavelets which exhibit near optimal time-frequency localization [17]. The third category are the biorthogonal wavelets which are constructed using two multiresolution analysis of L_2 instead of one, as in the two previous cases [6, 21]. The advantage of this last category is that the wavelet filters can be shorter; in particular, they can be both FIR and linear phase, which is typically not possible otherwise.

		intra-scale orthogonality	
		yes	no
inter-scale orthogonality	yes	orthogonal	semi-orthogonal
	no	shift-orthogonal	bi-orthogonal

Table I: Nomenclature of the various types of wavelet bases

One way to differentiate these various wavelet bases is to look at their orthogonality properties (cf . Table I). This classification naturally leads to the identification of one more type. These are the so-called *shift-orthogonal* wavelets which are orthogonal to their translates within the same scale, but not across scales. We presented the construction of an example using splines in a preliminary report [20].

0-8194-2213-4/96/$6.00

Downloaded from SPIE Digital Library on 19 Oct 2011 to 128.178.48.127. Terms of Use: http://spiedl.org/terms

In this paper, we extend this previous construction by considering more general spline spaces. A notable difference with our earlier example is that the present B-spline basis functions are not centered about the origin. This modification is necessary to cover the case of even degree splines, which leads to new wavelets that are anti-symmetric. We should emphasize that there is a practical motivation behind the present construction. Our choice of spline basis functions, especially the idea of using higher order of the synthesis side, is not arbitrary: we want our new wavelets to exhibit properties that are potentially useful for image coding and data compression [22]. First, they are very nearly orthogonal. Remember that orthogonality is required for the quantization error in the transformed domain to be equivalent to the error in the reconstructed image domain. Here, orthogonality with respect to shifts is consistent with the idea of independent channel processing (scalar quantization). We are giving up orthogonality with respect to dilations, but in a very controlled fashion by varying the angle between the analysis and synthesis spaces (cf. Section 2.2). Second, all basis functions are either symmetric or anti-symmetric. Consequently, these wavelet transforms can be computed using mirror signal extensions, one of the most efficient techniques for reducing boundary artifacts [15]. In contrast, non-linear phase wavelets such as Daubechies' can only be implemented using periodic signal extensions. Third, we will see that some of the wavelet filters decay faster than their orthogonal (Battle-Lemarié) counterparts. Hopefully, this should reduce the spreading of coding errors and ringing artifacts. Finally, our new wavelets have excellent approximation properties because they are constructed using very smooth functions (splines). This means that they will provide a very accurate low resolution approximation of smooth surfaces. Thus, we can expect most of the finer scale wavelet coefficients to be close to zero in slowly varying image regions, which is advantageous for zero-tree wavelet coding [12]. This last aspect of the problem is perhaps the strongest reason for using higher order splines on the synthesis side; a rigorous theoretical justification can be found elsewhere[14].

2. SPLINE SPACES

Our construction uses two spline multiresolution analyses of L_2. The analysis and synthesis functions will be splines of degree n_1 and n_2, respectively. Typically, we will select n_1=0 or n_1=1, and n_2>n_1. We will start by specifying these spline subspaces of L_2 explicitly.

2.1 Spline spaces

The spline multiresolution space of degree n at resolution i, V_i^n, is defined as

$$s_i(x) \in V_i^n \Leftrightarrow s_i(2^i x) \in V_0^n = \left\{ s_0(x) = \sum_{k \in Z} c(k) \varphi^n(x-k) \mid c \in l_2 \right\}, \tag{1}$$

where V_0^n is the basic space of splines of degree n, that is, the subspace of functions that are (n-1) continuously differentiable and are polynomial of degree n in each interval $[k, k+1)$ $k \in Z$. The generating function $\varphi^n(x)$ is Schoenberg's causal B-spline of degree n, which is obtained from the (n+1)-fold convolution of the indicator function in the unit interval [0,1). The B-spline of degree n satisfies the two-scale relation [19]

$$\varphi^n(x/2) = \sqrt{2} \sum_{k \in Z} h^n(k) \varphi^n(x-k), \tag{2}$$

where $h^n(k)$ is the binomial filter of order n+1 whose transfer function is

$$h^n(k) \quad \overset{z}{\longleftrightarrow} \quad H^n(z) = \sqrt{2} \cdot \left(\frac{1+z^{-1}}{2} \right)^{n+1}. \tag{3}$$

A crucial quantity in the specification of such a subspace is the autocorrelation sequence

$$a^n(k) = \langle \varphi^n(x-k), \varphi^n(x) \rangle = b^{2n+1}(k), \tag{4}$$

which is a sampled centered B-spline[18] of degree 2n+1 denoted by $b^{2n+1}(k)$. It can be shown that the discrete Fourier transform of the sequence $a^n(k)$ is bounded as follows:

Downloaded from SPIE Digital Library on 19 Oct 2011 to 128.178.48.127. Terms of Use: http://spiedl.org/terms

$$\forall \omega \in [0,2\pi), \qquad 0 < A_n \le \hat{a}^n(\omega) \le 1, \tag{5}$$

where $A_n = \sum_{k\in Z} \mathrm{sinc}^{2n+2}(\frac{1}{2}+k) = (2/\pi)^{2n+2} \cdot \sum_{k\in Z} (2k+1)^{-(2n+2)}$ is strictly positive. The constants $A=A_n$ and $B=1$ are the corresponding Riesz (or frame) bounds. This inequality ensures that the various spline spaces are well-defined (closed) subspaces of L_2 and that the construction actually makes sense.

Another important property is that splines of degree n have an order of approximation $L=n+1$. This is equivalent to say that for any L-times differentiable function f, we have the following error bound [13, 14]

$$\left\| f - P_i f \right\| \le C \cdot \left(2^{-i}\right)^L \cdot \left\| f^{(L)} \right\|, \tag{6}$$

where P_i represents any bounded projection operator (orthogonal or not) onto the spline space $V_i(\varphi)$ at resolution 2^{-i}, C is a constant that depends on φ^n and the type of projector, and $\left\| f^{(L)} \right\|$ is the L_2-norm of the Lth derivative of f. In other words, the error decays like $O(a^L)$ as the scale $a = 2^{-i}$ gets sufficiently small. Thus, we should expect higher order splines to result in a smaller approximation error, but the price to pay is an increase in complexity. The fact that the projector P_i does not need to be orthogonal also stresses the importance of the synthesis space which determines the rate of approximation. The exact type of projector will depend on our choice of analysis space. In the sequel, we will consider the oblique projector into $V_i^{n_2}$ in a direction perpendicular to $V_i^{n_1}$.

2.2 Angles between the spline spaces

Let φ_1 and φ_2 be any given two admissible analysis and synthesis scaling functions, respectively. Then, the largest angle θ_{12} between the analysis and synthesis spaces $V_i(\varphi_1)$ and $V_i(\varphi_2)$ is given by [16]

$$\cos\theta_{12} = \operatorname*{ess\,inf}_{\omega\in[0,\pi)} \frac{|\hat{a}_{12}(\omega)|}{\sqrt{\hat{a}_{11}(\omega)\cdot\hat{a}_{22}(\omega)}} \le 1, \tag{7}$$

where the functions $\hat{a}_{ij}(\omega)$ are the discrete Fourier transforms of the autocorrelation sequences

$$a_{ij}(k) = \langle \varphi_i(x-k), \varphi_j(x) \rangle = \left(\varphi_i^T * \varphi_j\right)(k), \quad (i,j=1,2), \tag{8},$$

where $\varphi_i^T(x) = \varphi_i(-x)$. In addition, the (oblique) projection into $V_i(\varphi_2)$ perpendicular to $V_i(\varphi_1)$ is well defined if and only if $\cos\theta_{12} > 0$ (that is, if $-\pi/2 < \theta_{12} < \pi/2$) [3].

In our case, we select $\varphi_1 = \varphi^{n_1}$ and $\varphi_2 = \varphi^{n_2}$. Simplifying the notation and dropping the order parameter n, we can determine the analysis and synthesis autocorelations sequences

$$a_{11}(k) = \varphi^{2n_1+1}\left(k + \frac{2n_1+1}{2}\right) \tag{9}$$

$$a_{22}(k) = \varphi^{2n_2+1}\left(k + \frac{2n_2+1}{2}\right) \tag{10}$$

which is equivalent to (4) with $n = n_1$ and $n = n_2$, respectively. Similarly, it is not difficult to show that the cross-correlation is given by

$$a_{12}(k) = \varphi^{n_1+n_2+1}\left(k - \frac{(n_2-n_1)}{2}\right). \tag{11}$$

These are all finite sequences that can be determined numerically for any given n_1 and n_2. It is then straightforward to determine the angle between the various spline spaces using (7). The result of these calculations for all combination of splines up to the degree 7 are given in Table II. In the present context, these worst case cosine values are useful indicators of the loss of orthogonality across scale for our hybrid spline wavelet transforms. In general, the angle is less then $\pi/2$ in absolute value (i.e., $\cos\theta_{12} > 0$) only when $(n_2 - n_1)$ is even, that is, when the degrees n_1 and n_2 are both odd, or both even.

Downloaded from SPIE Digital Library on 19 Oct 2011 to 128.178.48.127. Terms of Use: http://spiedl.org/terms

n_1 \ n_2	0	1	2	3	4	5	6	7
0	1	0	0.8729	0	0.8162	0	0.7837	0
1		1	0	0.9709	0	0.9374	0	0.9103
2			1	0	0.9857	0	0.9634	0
3				1	0	0.9911	0	0.9751
4					1	0	0.9939	0
5						1	0	0.9955
6							1	0
7								1

Table II: $\cos\theta_{12}$ between the splines space $V_0(\varphi^{n_1})$ and $V_0(\varphi^{n_2})$.

3. SHIFT-ORTHOGONAL SCALING FUNCTIONS AND WAVELETS

3.1 Construction of dual spline scaling functions

Our basic approximation (or synthesis) space is $V_0^{n_2}$. As mentioned previously, the parameter important for performance is the order of the representation $L=n_2+1$, which is one more than the degree. The corresponding orthogonal generating function is the Battle-Lemarié scaling function which can be expressed as [19]

$$\phi(x)=\sum_{k\in Z}\left(a_{22}\right)^{-1/2}(k)\varphi^{n_2}(x-k), \tag{12}$$

where $\left(a_{22}\right)^{-1/2}(k) \xleftrightarrow{Fourier} 1/\sqrt{\hat{a}_{22}(\omega)}$ denotes the square-root convolution inverse of the symmetric sequence $a_{22}(k)$. Here, we will only consider the symmetrical square-root inverse. In principle, there are many other equivalent solutions which only differ in terms of a phase factor.

Instead of performing a decomposition in $V_0^{n_2}$ by using an orthogonal projection as in the Battle-Lemarié case[11], we use an oblique projection perpendicular to $V_0^{n_1}$, where n_1 is typically a spline of degree 0 or 1, depending on the parity of n_2. We may also consider higher order analysis spaces, but our motivation here is to have the simplest possible analysis functions. The corresponding (unique) dual function $\tilde{\phi}(x)\in V_0^{n_1}$ must satisfy the biorthogonality constraint $\langle\phi(x),\tilde{\phi}(x-k)\rangle=\delta[k]$, where $\delta[k]$ is the discrete unit impulse [16]. This leads to the following characterization

$$\tilde{\phi}(x)=\sum_{k\in Z}\left(a_{22}\right)^{1/2} * \left(a_{12}^T\right)^{-1}(k)\ \varphi^{n_1}(x-k), \tag{13}$$

where $\left(a_{12}^T\right)^{-1}(k)$ is the convolution inverse of the cross-correlation sequence $a_{21}(k)=a_{12}^T(k)=\langle\varphi^{n_2}(x-k),\varphi^{n_1}(x)\rangle$. Note that all the required inverse filters in (12) and (13) are well-defined because of the stability conditions (5) and $\cos\theta_{12}>0$.

Unlike ϕ, the dual function $\tilde{\phi}$ is not orthogonal to its own shifts. In fact, we can easily compute its sampled auto-correlation sequence

$$a_{\tilde{\phi}}(k)=\langle\tilde{\phi}(x-k),\tilde{\phi}(x)\rangle=\left(a_{22} * \left(a_{12} * a_{12}^T\right)^{-1} * a_{11}\right)(k). \tag{14}$$

If we express this relation in the Fourier domain and use (7), we obtain the following frame inequality

$$1\le\hat{a}_{\tilde{\phi}}(\omega)=\left(\frac{\hat{a}_{22}(\omega)\cdot\hat{a}_{11}(\omega)}{\left|\hat{a}_{12}(\omega)\right|^2}\right)\le\frac{1}{\left(\cos\theta_{12}\right)^2}, \tag{15}$$

which provides an interesting geometrical connection. In other words, we have full orthogonality if and only if $\cos\theta_{12}=1$, or equivalently, when φ_1 and φ_2 generate the same space.

Downloaded from SPIE Digital Library on 19 Oct 2011 to 128.178.48.127. Terms of Use: http://spiedl.org/terms

Having defined these new basis functions, we can now write the projection P_i of a function $f \in L_2$ into $V_i^{n_2}$ perpendicular to $V_i^{n_1}$ as

$$P_i f(x) = \sum_{k \in Z} \langle f, \tilde{\phi}_{i,k} \rangle \ \phi_{i,k} \tag{16}$$

where we use the standard short form notation $\phi_{i,k} = 2^{-i/2}\phi(x/2^i - k)$.

3.2 Construction of shift-orthogonal spline wavelets

We now consider the characterization of the corresponding wavelets at resolution level i=1. The synthesis wavelet $\psi(x/2)$ must satisfy the following conditions:

(*i*) $\psi(x/2) \in V_0^{n_2}$ (i.e., $\psi(x/2)$ is a spline of degree n_2);

(*ii*) $\langle \psi(x/2), \varphi^{n_1}(x/2 - k) \rangle = 0$ because $\psi(x/2)$ is perpendicular to $V_1^{n_1}$;

(*iii*) $\langle 2^{-1/2}\psi(x/2), 2^{-1/2}\psi(x/2 - k) \rangle = \delta[k]$ (intra-scale orthogonality).

It turns out that there is a unique function ψ that verifies all those conditions; it is given by

$$\psi(x/2) = \sum_{k \in Z} [p]_{\uparrow 2} * q(k) \ \varphi^{n_2}(x - k), \tag{17}$$

where the sequences q and p are defined as follows

$$q(k+1) = (-1)^k \cdot \left(h_1^T * a_{12}\right)(k) \tag{18}$$

$$p(k) = \sqrt{2} \cdot \left(\left[q * q^T * a_{22} \right]_{\downarrow 2} \right)^{-1/2}(k). \tag{19}$$

The operators $[\bullet]_{\uparrow 2}$ and $[\bullet]_{\downarrow 2}$ denote up-sampling and down-sampling by a factor of two, respectively, and $q^T(k) = q(-k)$. The sequence $h_1(k)$ is the binomial filter in (3) with n=n_1; the corresponding correlation sequences are given by (10) and (9). Note that this wavelet is nothing else as the orthogonalized version of the basic wavelet defined by Abry and Aldroubi [2], which is given by (17) with p=identity. The framebound conditions on the basic wavelet imply that the operator p is a well-defined convolution operator from l_2 into l_2.

The dual analysis wavelet $\tilde{\psi}(x/2)$ must satisfy a similar set of conditions:

(*i*) $\tilde{\psi}(x/2) \in V_0^{n_1}$ (i.e., $\tilde{\psi}(x/2)$ is a spline of degree n_1);

(*ii*) $\langle \tilde{\psi}(x/2), \varphi^{n_2}(x/2 - k) \rangle = 0$ because $\tilde{\psi}(x/2)$ is perpendicular to $V_1^{n_2}$;

(*iii*) $\langle 2^{-1/2}\tilde{\psi}(x/2), 2^{-1/2}\psi(x/2 - k) \rangle = \delta[k]$ (bi-orthogonality).

After some algebraic manipulations, we obtain the similar expression

$$\tilde{\psi}(x/2) = \sum_{k \in Z} [\tilde{p}]_{\uparrow 2} * \tilde{q}(k) \ \varphi^{n_1}(x - k), \tag{20}$$

where

$$\tilde{q}(k+1) = (-1)^k \cdot \left(h_2^T * a_{12}^T\right)(k) \tag{21}$$

$$\tilde{p}(k) = 2 \cdot \left(p * \left[q^T * \tilde{q} * a_{12}^T \right]_{\downarrow 2} \right)^{-1}(k) \tag{22}$$

with p and q defined in (19) and (18); the sequences h_2^T and a_{12}^T are the time-reversed version of binomial filter in (3) with n=n_2 and the cross-correlation sequence (9). When the maximum angle θ_{12} between the analysis and synthesis spaces $V_0^{n_1}$ and $V_0^{n_2}$ is less than 90 degrees (cf. Table II), the corresponding wavelet subspaces and oblique projection operators are well-defined [3]. Hence, the convolution and square-root inverses in (19) and (22) are well-posed, and the resulting digital filters p and $\tilde{p}$ are stable and invertible. The corresponding dual pairs of scaling functions and wavelets for n_1=0 and n_2=2 are shown in Fig. 1. One can observe that the basis functions are piecewise constant on the analysis side and piecewise quadratic with a first order of continuity on the synthesis side. Interestingly, the analysis function $\tilde{\phi}$ has a very fast decay and is reasonably close to a B-spline of degree 0. Also note that for the particular case $n_1 = n_2$, the present construction yields the Battle-Lemarié spline wavelets which are completely orthogonal [5, 10].

Downloaded from SPIE Digital Library on 19 Oct 2011 to 128.178.48.127. Terms of Use: http://spiedl.org/terms

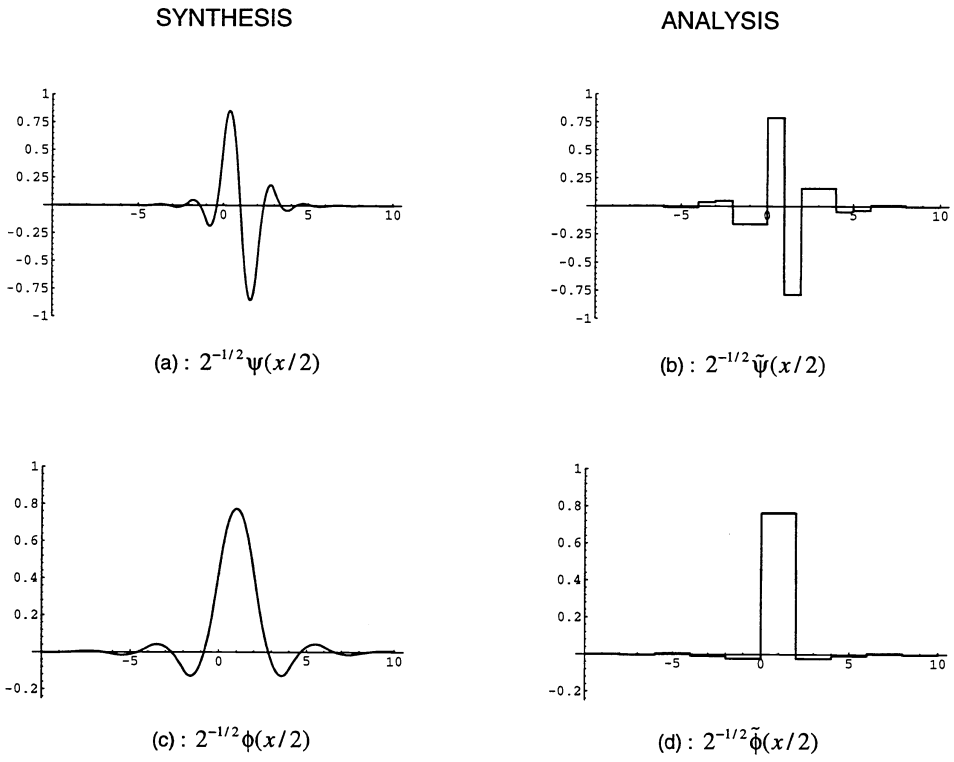

Fig. 1 : Dual sets of quadratic spline and piecewise constant wavelets and scaling functions at the first resolution level : (a) shift-orthogonal quadratic spline wavelet ;(b) dual piecewise constant wavelet; (c) orthogonal quadratic spline Battle-Lemarié scaling function; and (d) dual piecewise constant analysis scaling function. The basis functions in (a) and (b) (resp., (c) and (d)) are quadratic splines with knots at the integers (resp., at the even integers).

4. WAVELET TRANSFORM AND FILTERBANK ALGORITHM

Let $W_i^{n_2}$ be the complementary wavelet space of $V_i^{n_2}$ in $V_{i-1}^{n_2}$ but perpendicular to $V_i^{n_1}$; i.e., $V_{i-1}^{n_2} = W_i^{n_2} + V_i^{n_2}$ with $W_i^{n_2} \perp V_i^{n_1}$. It is not difficult to show that $\{\psi_{i,k} = 2^{-i/2}\psi(x/2^{-i} - k)\}_{k\in Z}$ is an orthogonal basis of $W_i^{n_2}$. Since it is well known that $\bigcup_{i\in Z} V_i^{n_2}$ is dense in L_2, it follows that the set $\{\psi_{i,k}\}_{(i,k)\in Z^2}$ is an unconditional basis of L_2, and that every function $f \in L_2$ can be represented by its shift-orthogonal wavelet expansion

$$f(x) = \sum_{i\in Z} \sum_{k\in Z} \langle f, \tilde{\psi}_{i,k} \rangle \psi_{i,k}. \qquad (23)$$

The special feature of this decomposition is that the basis functions are orthogonal with respect to shifts (index k), but not across scales or dilations (index i). We should note, however, that the residual correlations across scales should not be too significant because the angles between the various spline spaces are relatively small (cf. Table II). For these reasons, we can expect the shift-orthogonal decomposition (23) to provide essentially the same type of energy compaction as the corresponding orthogonal Battle-Lemarié wavelet transform.

The wavelet transform (23) can be implemented iteratively using a standard tree-structured perfect reconstruction filterbank[22]. The corresponding symmetric analysis and synthesis filters $(\tilde{h}, \tilde{g})$ and (h, g), respectively, are defined as follows:

Downloaded from SPIE Digital Library on 19 Oct 2011 to 128.178.48.127. Terms of Use: http://spiedl.org/terms

$$\begin{cases} \tilde{h}(k) = \frac{1}{\sqrt{2}}\langle \tilde{\phi}(x/2), \phi(x+k) \rangle \\ \tilde{g}(k) = \frac{1}{\sqrt{2}}\langle \tilde{\psi}(x/2), \phi(x+k) \rangle \\ h(k) = \frac{1}{\sqrt{2}}\langle \phi(x/2), \tilde{\phi}(x-k) \rangle \\ g(k) = \frac{1}{\sqrt{2}}\langle \psi(x/2), \tilde{\phi}(x-k) \rangle \end{cases} . \tag{24}$$

The easiest way to determine these filters is to perform the appropriate change of coordinate system and express $\phi(x/2)$ and $\psi(x/2)$ (resp., $\tilde{\phi}(x/2)$ and $\tilde{\psi}(x/2)$) in terms of the integer shifts of ϕ (resp., $\tilde{\phi}$). This provides an explicit characterization of their impulse response in the signal domain. We have chosen here to present frequency domain formulas because these turn out to be the most useful in practice. Our results are summarized as follows:

$$H(e^{j\omega}) := \hat{h}(\omega) = \hat{h}_2(\omega) \cdot \sqrt{\frac{\hat{a}_{22}(\omega)}{\hat{a}_{22}(2\omega)}} \tag{25}$$

$$\tilde{H}(e^{j\omega}) := \hat{\tilde{h}}(\omega) = \overline{\hat{h}_1(\omega)} \cdot \frac{\hat{a}_{12}(\omega)}{\hat{a}_{12}(2\omega)} \cdot \sqrt{\frac{\hat{a}_{22}(2\omega)}{\hat{a}_{22}(\omega)}} \tag{26}$$

$$G(e^{j\omega}) := \hat{g}(\omega) = \frac{1}{\sqrt{2}} e^{-j\omega} \cdot \overline{\hat{h}_1(\omega+\pi)} \cdot \hat{p}(2\omega) \cdot \hat{a}_{12}(\omega+\pi) \cdot \sqrt{\hat{a}_{22}(\omega)} \tag{27}$$

$$\tilde{G}(e^{j\omega}) := \hat{\tilde{g}}(\omega) = e^{j\omega} \cdot \frac{\sqrt{2} \cdot \hat{h}_2(\omega+\pi)}{\hat{a}_{12}(2\omega)\sqrt{\hat{a}_{22}(\omega)}} \cdot \frac{1}{\hat{p}(2\omega)}, \tag{28}$$

where the auxiliary filters $\tilde{p}(2\omega)$ and $\hat{q}_a(\omega)$ are defined as follows

$$\hat{p}(2\omega) = \frac{2}{\sqrt{\hat{q}_a(\omega) + \hat{q}_a(\omega+\pi)}} \tag{29}$$

$$\hat{q}_a(\omega) = \left|\hat{h}_1(\omega+\pi)\right|^2 \cdot \left|\hat{a}_{12}(\omega+\pi)\right|^2 \cdot \hat{a}_{22}(\omega). \tag{30}$$

All filters are infinite but decay exponentially fast.

In order to compute a truncated version of a filter's impulse response, the simplest approach is to evaluate its transfer function at the discrete frequencies $\omega_i = 2\pi i/N$, $i = 0,\ldots,N-1$, where N is chosen sufficiently large to avoid aliasing in the signal domain. The impulse response is then determined by using an N-point inverse FFT. The first 20 filter coefficients for n_1=1 and n_2=3 (cubic splines) are given in Table III. The lowpass filter h is the same as the Battle-Lemarié filter described by Mallat [11]. Interestingly, the wavelet synthesis filter g decays significantly faster, and turns out to be very similar to a Battle-Lemarié filter of degree 1 (n=1), which is also given for comparison.

4. CONCLUSION

We have presented a new class of hybrid spline wavelet transforms. The motivation behind this proposal was to use lower order analysis functions, while essentially preserving the approximation and orthogonality properties of higher order Battle-Lemarié wavelets. An important consideration was also to design wavelets that are either symmetric or anti-symmetric, a feature that is desirable in many applications. In contrast with previous semi- and bi-orthogonal constructions, we have only relaxed the orthogonality constraint in-between resolution levels. The basis functions are still orthogonal within a given wavelet channel (or scale), a property that is quite desirable for quantization purposes. The advantage over the Battle-Lemarié family is that the wavelet synthesis filter decays substantially faster, a property that could be useful for reducing ringing artifacts in coding

Downloaded from SPIE Digital Library on 19 Oct 2011 to 128.178.48.127. Terms of Use: http://spiedl.org/terms

applications. All the underlying basis functions (including duals) have been characterized explicitly in the time domain (polynomial spline representation). Such direct formulas are in general not available for other wavelet bases, except for the class of semi-orthogonal splines considered by us earlier [19].

k	$\tilde{h}(k)$	$\tilde{g}(k-1)$	$h(k)$	$g(k+1)$	Battle-Lemarié n=1
0	0.82382	0.772627	0.76613	0.8166	0.817646
±1	0.399749	-0.435933	0.433923	-0.398208	-0.397297
±2	-0.073438	-0.0543491	-0.0502017	-0.0688421	-0.069101
±3	-0.0559962	0.113795	-0.110037	0.0532619	0.0519453
±4	0.0174812	0.0321753	0.0320809	0.0174535	0.016971
±5	0.0118749	-0.0443877	0.0420684	-0.0104416	-0.00999059
±6	-0.00187877	-0.0152844	-0.0171763	-0.00411726	-0.00388326
±7	-0.00235935	0.0184738	-0.0179823	0.00228748	0.00220195
±8	-0.00130068	0.00673909	0.00868529	0.000960346	0.000923371
±9	0.000166395	-0.00785314	0.00820148	-0.000556564	-0.000511636
±10	0.0013526	-0.00292239	-0.00435384	-0.000247084	-0.000224296
±11	0.000257732	0.00336119	-0.00388243	0.00013056	0.000122686
±12	-0.000916596	0.00126143	0.00218671	0.0000590167	0.0000553563
±13	-0.000236368	-0.00144343	0.00188213	-0.0000338138	-0.0000300112
±14	0.000534489	-0.000543627	-0.00110374	-0.0000157658	-0.0000138188
±15	0.000155065	0.000620628	-0.000927199	$8.13544\ 10^{-6}$	$7.44435\ 10^{-6}$
±16	-0.000292241	0.000234175	0.000559937	$3.80939\ 10^{-6}$	$3.4798\ 10^{-6}$
±17	-0.0000892527	-0.000267052	0.000462115	$-2.17513\ 10^{-6}$	$-1.86561\ 10^{-6}$
±18	0.000153515	-0.000100845	-0.000285384	$-1.04198\ 10^{-6}$	$-8.82258\ 10^{-7}$
±19	0.0000484485	0.000114942	-0.000232347	$5.29128\ 10^{-7}$	$4.71223\ 10^{-7}$
±20	-0.0000788157	0.000043426	0.000146042	$2.52873\ 10^{-7}$	$2.24913\ 10^{-7}$

Table III: Filter coefficients for the cubic spline shift-orthogonal wavelet transform with $n_1 = 1$ and $n_2 = 3$. The filters are all symmetric. The last column displays the Battle-Lemarié wavelet filter of degree one ($n_1 = n_2 = 1$).

References

1. P. Abry and A. Aldroubi, "Designing multiresolution analysis-type wavelets and their fast algorithms", *J. Fourier Analysis and Applications*, Vol. 2, No. 2, pp. 135-159, 1995.
2. P. Abry and A. Aldroubi, "Semi- and bi-orthogonal MRA-type wavelet design and their fast algorithms", *Proc. SPIE Conf Wavelet Applications in Signal and Image Processing III*, San Diego, CA, pp. 452-463, July 9-14, 1995.
3. A. Aldroubi, "Oblique projections in atomic spaces", *Proc. Amer. Math. Soc.*, Vol. 124, No. 7, pp. 2051-2060, July 1996.
4. A. Aldroubi and M. Unser, "Families of multiresolution and wavelet spaces with optimal properties", *Numerical Functional Analysis and Optimization*, Vol. 14, No. 5-6, pp. 417-446, 1993.
5. G. Battle, "A block spin construction of ondelettes. Part I: Lemarié functions", *Commun. Math. Phys.*, Vol. 110, pp. 601-615, 1987.
6. A. Cohen, I. Daubechies and J.C. Feauveau, "Bi-orthogonal bases of compactly supported wavelets", *Comm. Pure Appl. Math.*, Vol. 45, pp. 485-560, 1992.
7. I. Daubechies, "Orthogonal bases of compactly supported wavelets", *Comm. Pure Appl. Math.*, Vol. 41, pp. 909-996, 1988.
8. I. Daubechies, *Ten lectures on wavelets*, Society for Industrial and Applied Mathematics, Philadelphia, PA, 1992.

Downloaded from SPIE Digital Library on 19 Oct 2011 to 128.178.48.127. Terms of Use: http://spiedl.org/terms

9. B. Jawerth and W. Sweldens, "An overview of wavelet based multiresolution analyses", *SIAM Review*, Vol. 36, No. 3, pp. 377-412, September 1994.
10. P.-G. Lemarié, "Ondelettes à localisation exponentielles", *J. Math. pures et appl.*, Vol. 67, No. 3, pp. 227-236, 1988.
11. S.G. Mallat, "A theory of multiresolution signal decomposition: the wavelet representation", *IEEE Trans. Pattern Anal. Machine Intell.*, Vol. PAMI-11, No. 7, pp. 674-693, 1989.
12. J. Shapiro, "Embedded image coding using zerotrees of wavelet coefficients", *IEEE Transactions on Acoustics, Speech and Signal Processing*, Vol. 41, No. 12, pp. 3445-3462, December 1993.
13. G. Strang and G. Fix, "A Fourier analysis of the finite element variational method", in: *Constructive Aspect of Functional Analysis*, Edizioni Cremonese, Rome, 1971, pp. 796-830.
14. M. Unser, "Approximation power of biorthogonal wavelet expansions", *IEEE Trans. Signal Processing*, Vol. 44, No. 3, pp. 519-527, March 1995.
15. M. Unser, "A practical guide to the implementation of the wavelet transform", in: A. Aldroubi and M. Unser, ed., *Wavelets in Medicine and Biology*, CRC Press, Boca Raton, FL, 1996, pp. 37-73.
16. M. Unser and A. Aldroubi, "A general sampling theory for non-ideal acquisition devices", *IEEE Trans. Signal Processing*, Vol. 42, No. 11, pp. 2915-2925, November 1994.
17. M. Unser, A. Aldroubi and M. Eden, "On the asymptotic convergence of B-spline wavelets to Gabor functions", *IEEE Trans. Information Theory*, Vol. 38, No. 2, pp. 864-872, March 1992.
18. M. Unser, A. Aldroubi and M. Eden, "B-spline signal processing. Part I: theory", *IEEE Trans. Signal Processing*, Vol. 41, No. 2, pp. 821-833, February 1993.
19. M. Unser, A. Aldroubi and M. Eden, "A family of polynomial spline wavelet transforms", *Signal Processing*, Vol. 30, No. 2, pp. 141-162, January 1993.
20. M. Unser, P. Thévenaz and A. Aldroubi, "Shift-orthogonal wavelet bases using splines", *IEEE Signal Processing Letters*, Vol. 3, No. 3, pp. 85-88, March 1996.
21. M. Vetterli and C. Herley, "Wavelets and filter banks: theory and design", *IEEE Trans. Signal Processing*, Vol. 40, No. 9, pp. 2207-2232, September 1992.
22. M. Vetterli and J. Kovacevic, *Wavelets and Subband Coding*, Prentice Hall, Englewood Cliffs, NJ, 1995.

Downloaded from SPIE Digital Library on 19 Oct 2011 to 128.178.48.127. Terms of Use: http://spiedl.org/terms